Acta Crystallographica Section F
Structural Biology and Crystallization Communications
ISSN 1744-3091

Overproduction, purification and preliminary X-ray diffraction analysis of YncE, an iron-regulated Sec-dependent periplasmic protein from *Escherichia coli*

Aisha Baba-Dikwa,[a] Darren Thompson,[b]‡ Nick J. Spencer,[b] Simon C. Andrews[a] and Kimberly A. Watson[a,b]*

[a]School of Biological Sciences, University of Reading, Whiteknights Campus, Reading, Berkshire RG6 6AS, England, and [b]Structural Biology Unit, The BioCentre, University of Reading, Whiteknights Campus, Reading, Berkshire RG6 6AS, England

‡ Current address: Biochemistry, School of Life Sciences, John Maynard-Smith Building, University of Sussex, Falmer, Brighton BN1 9QG, England.

Correspondence e-mail: k.a.watson@reading.ac.uk

Received 25 July 2008
Accepted 15 September 2008

The *yncE* gene of *Escherichia coli* encodes a predicted periplasmic protein of unknown function. The gene is de-repressed under iron restriction through the action of the global iron regulator Fur. This suggests a role in iron acquisition, which is supported by the presence of the adjacent *yncD* gene encoding a potential TonB-dependent outer-membrane transporter. Here, the preliminary crystallographic structure of YncE is reported, revealing that it consists of a seven-bladed β-propeller which resembles the corresponding domain of the 'surface-layer protein' of *Methanosarcina mazei*. A full structure determination is under way in order to provide insight into the function of this protein.

1. Introduction

The *yncE* gene encoding the 327-residue YncE protein was identified in *Escherichia coli* during studies on global iron-dependent gene expression, where it was found to be up to 18-fold repressed by the Fe^{2+}–Fur complex (McHugh *et al.*, 2003). A Fur-box-like sequence is suitably located upstream of the *yncE* promoter, which is consistent with direct transcriptional repression by Fe^{2+}–Fur (McHugh *et al.*, 2003). YncE possesses a putative N-terminal signal sequence suggestive of export; consistent with this, it has been shown to be secreted into the periplasm *via* the Sec-dependent pathway (McHugh *et al.*, 2003; Baars *et al.*, 2006). *yncE* is adjacent to the divergently transcribed *yncD* gene that encodes a potential TonB-dependent outer-membrane (OM) receptor that is possibly involved in the translocation of iron complexes across the outer membrane (McHugh *et al.*, 2003). In addition, the homologous TieB protein (with a putative role in enterotoxin production) of enteroinvasive *E. coli* strain O164 is apparently encoded as part of the Fe^{2+}–Fur repressed *cjrABC-senB* operon (Šmajs & Weinstock, 2001; Nataro *et al.*, 1995). This operon also specifies a TonB-dependent OM receptor as well as a TonB homologue, although it is functionally undefined except for a role in colicin Js sensitivity. These observations, together with the iron regulation and periplasmic location, are suggestive of an iron-transport function for YncE.

The primary structure of YncE suggests that it is composed of seven tandemly repeated motifs (~40 amino acids, four β-strands) forming a so-called 'YVTN β-propeller' (as defined in the InterPro database). Similarly repeated motifs are found in ~200 functionally undefined bacterial and archaeal proteins in the sequence databases. For bacteria, the YVTN β-propeller proteins all consist of a single YVTN β-propeller domain. However, archaeal YVTN β-propeller proteins are often multidomain proteins containing, for instance, TolB-like, multiple PKD-like, peptidase-like or pectinase-like domains together with one or two YVTN β-propeller domains. The archaeal species *Methanosarcina mazei* and *M. acetivorans* each have more than ten genes each that encode YVTN β-propeller domains and all are of unknown function. The structure of the YVTN β-propeller domain of the multidomain 'surface-layer protein' of *M. mazei* has been determined, revealing a seven-bladed β-propeller structure (Jing *et al.*, 2002). This protein currently represents the sole

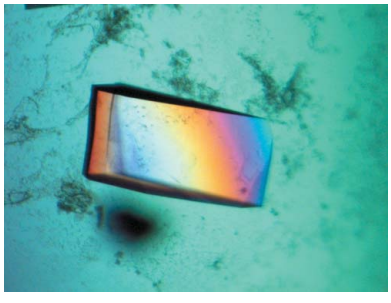

structurally defined member of the YVTN β-propeller family of proteins.

This work reports the overproduction, purification, crystallization and preliminary X-ray crystallographic analysis of YncE from *E. coli*.

2. Material and methods

2.1. Protein preparation

The *yncE* gene (GeneID 946006; UniProtKB/Swiss-Prot entry P76116) was PCR-amplified using the high-fidelity DNA polymerase Accuzyme (Bioline) and cloned into the Champion pET Directional TOPO overexpression vector (Invitrogen) to generate plasmid pET*yncE*-His$_6$. The forward PCR primer was designed such that the initiating ATG codon of *yncE* directly followed the CACC motif required for TOPO cloning. The reverse PCR primer was designed to exclude the natural stop codon of *yncE*, thus enabling the production of an in-frame translational fusion between *yncE* and the downstream vector-encoded V5 epitope and the His$_6$ tag.

Overproduction of YncE-His$_6$ was achieved using BL21 (DE3) (pET*yncE*-His$_6$) grown in L-broth plus ampicillin (100 µg ml^{-1}) at 310 K, with the addition of 1 m*M* isopropyl β-D-1-thiogalactopyranoside (IPTG) when the culture achieved an optical density of 0.5 at 650 nm. IPTG-induced cells were grown for a further 4 h, harvested, resuspended in 3 ml of binding buffer [25 m*M* HEPES pH 7.4, 10 m*M* imidazole, 150 m*M* NaCl, 20 m*M* mannitol, 10%(*v*/*v*) glycerol] per gram of cell weight and lysed at 76 MPa with a French pressure cell. YncE-His$_6$ was then purified from the soluble supernatant by chromatography with an Ni^{2+}-charged HiTrap Affinity resin column and a linear gradient of 0.01–0.5 *M* imidazole in binding buffer. The resulting protein was >95% pure as judged by SDS–PAGE analysis (Fig. 1) and was dialysed against storage buffer [50 m*M* HEPES pH 7.4, 100 m*M* NaCl, 10%(*v*/*v*) glycerol] and concentrated using a Vivaspin system (10 kDa cutoff; Vivascience) to 3.4 mg ml^{-1} prior to storage at 193 K.

2.2. Crystallization

Purified YncE-His$_6$ was buffer-exchanged and concentrated to 15 mg ml^{-1} in 50 m*M* HEPES pH 7.4 in preparation for crystallization trials. Initial crystallization screening was performed manually using the sitting-drop vapour-diffusion method in 24-well Linbro plates against the following commercial screens at 291 K: Crystal Structure Screens I and II, Structure Screens I and II, Stura Footprint Screen, Macrosol I and II and PEG/Ion Screen (all from Molecular Dimensions Ltd). The drop size was 2 µl plus 2 µl in all cases.

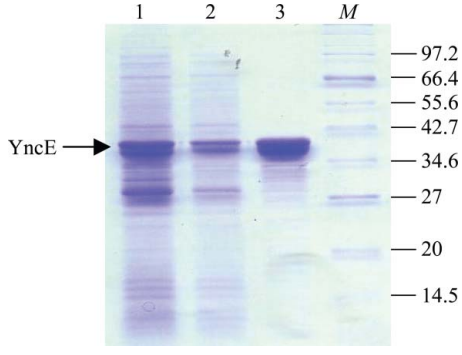

Figure 1
Purification of YncE-His$_6$. SDS–PAGE (12% acrylamide) analysis of samples at different stages of YncE-His$_6$ purification. Lane 1, crude whole-cell extract following cell lysis; lane 2, soluble cell extract derived from the crude extract by centrifugation; lane 3, YncE-His$_6$ after purification by Ni^{2+}-affinity chromatography; lane *M*, molecular-weight markers (sizes indicated in kDa). Approximately 50, 25 and 5 µg of protein were loaded in lanes 1, 2 and 3, respectively.

Table 1
Data-collection and processing statistics for YncE-His$_6$.

Values in parentheses are for the highest resolution shell.

Synchrotron beamline	SRS PX9.6
Wavelength (Å)	0.87
Space group	$P2_1$
Unit-cell parameters (Å, °)	a = 69.7, b = 108.8, c = 85.3, β = 105.03
Resolution range (Å)	50.0–2.1 (2.21–2.10)
$R_{\rm merge}$†	0.107 (0.396)
No. of observations	254997 (36245)
No. of unique reflections	71543 (10361)
Mean $I/\sigma(I)$‡	13.5 (4.0)
Completeness (%)	99.8 (99.4)
Multiplicity	3.6 (3.5)
Solvent content (%)	44.9
Molecules per ASU	4

† $R_{\rm merge} = \sum_{hkl}\sum_i |I_i(hkl) - \langle I(hkl)\rangle| / \sum_{hkl}\sum_i I_i(hkl)$, where the outer summation is over all unique reflections with multiple observations and the inner summation is over all observations of each reflection. ‡ $\sigma(I)$ is the standard deviation of I.

2.3. Diffraction analysis

The YncE-His$_6$ crystals could be sufficiently cryoprotected in the mother-liquor solution [which contained 22%(*v*/*v*) PEG 550 MME] and therefore could be flash-cooled directly from the hanging drop. Intensity data were collected on an ADSC Quantum 4 CCD detector at 100 K on the macromolecular beamline PX9.6 at SRS Daresbury, UK. Data were integrated and scaled using the programs *MOSFLM* v.6.2.4 (Leslie, 1992) and *SCALA* (Evans, 1997), respectively, from the *CCP*4 program package (Collaborative Computational Project, Number 4, 1994).

2.4. Phasing

According to *WU-Blast*2 analysis, the protein that shared the highest amino-acid sequence identity (25% over 183 residues) for which a structure has been reported was found to be the tandem YVTN β-propeller domain from the archaeal surface-layer protein (PDB code 1l0q). The *CCP*4 program *CHAINSAW* was used to create an initial model based on 1l0q, pruning the nonconserved residues to the last common atom. The resulting model, consisting of

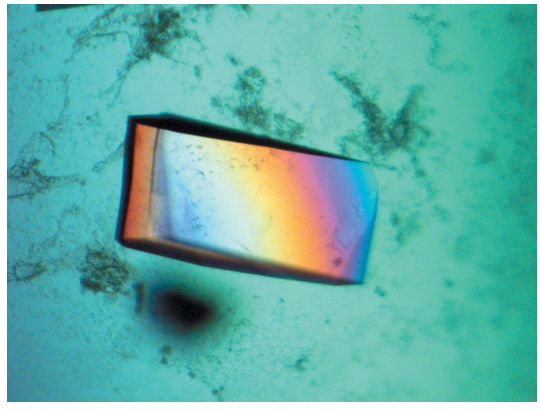

Figure 2
Crystallization of YncE-His$_6$ produced large (typical dimensions 0.3 × 0.15 × 0.05 mm) diffraction-quality crystals from optimization of Stura Footprint Screen condition C1 [0.1 *M* HEPES pH 8.2, 30%(*v*/*v*) PEG 550 MME]. Optimal conditions for YncE-His$_6$ were found to be 0.1 *M* Tris pH 7.5, 22%(*v*/*v*) PEG 550 MME. The drop size was 2 µl plus 2 µl and the protein concentration was 8 mg ml^{-1}.

residues 22–323 of YncE-His$_6$, was used as the search model for molecular replacement against all data between 50 and 3.0 Å resolution using *Phaser* (McCoy *et al.*, 2007).

3. Results and discussion

The YncE protein of *E. coli* was purified to homogeneity and crystallized for structure determination. From the 480 conditions screened, optimization of Stura Footprint Screen condition C1 [0.1 *M* Na HEPES pH 8.2, 30%(*v*/*v*) PEG 550 MME] gave rise to large single crystals of typical dimensions 0.30 × 0.15 × 0.05 mm (Fig. 2). The final optimized conditions for reliable production of diffraction-quality crystals of YncE-His$_6$ were 0.1 *M* Tris pH 7.5, 22%(*v*/*v*) PEG 550 MME. The crystals appeared within two weeks. The crystals diffracted to 1.9 Å resolution and belonged to space group $P2_1$, with unit-cell parameters a = 69.7, b = 108.8, c = 85.3 Å, β = 105.03°, giving rise to four monomers in the asymmetric unit with a solvent content of 48%. A typical image showing diffraction intensities to 2.1 Å resolution for native YncE-His$_6$ (PX9.6, SRS Daresbury) is shown in Fig. 3 and the data-processing statistics are presented in Table 1.

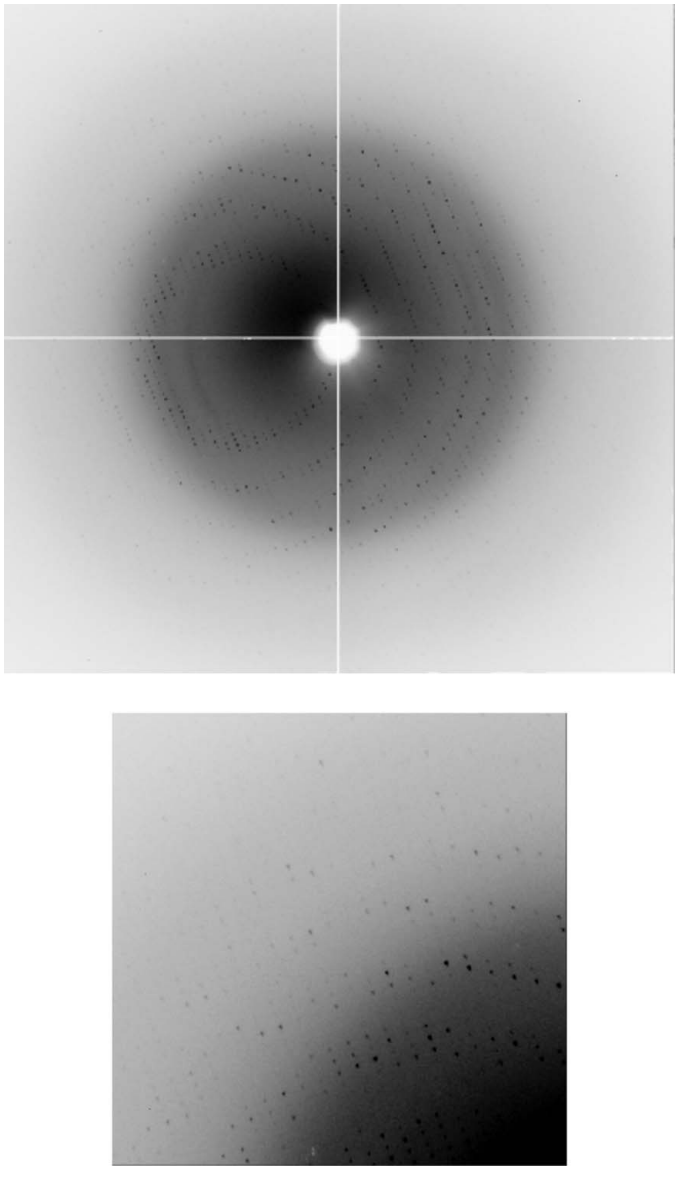

Figure 3
Typical diffraction image obtained for YncE-His$_6$ recorded at station PX9.6, SRS Daresbury. The enlarged region is taken from the upper-left corner of the image, showing diffraction close to the edge of the detector. The resolution at the edge is 2.0 Å.

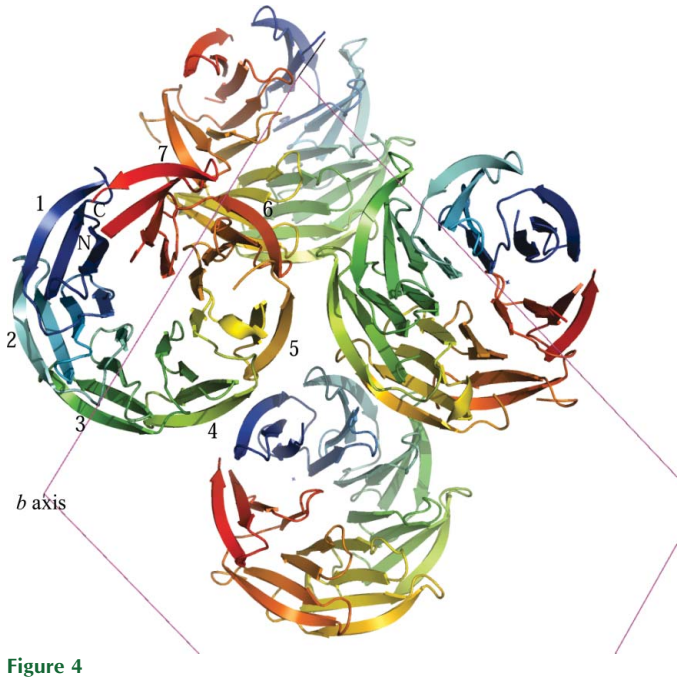

Figure 4
The molecular-replacement model from *Phaser* of YncE-His$_6$ (residues 22–323) exhibits seven four-stranded β-sheets forming a seven-bladed β-propeller fold. The seven blades of the monomer (numbered 1–7) are shown colour coded from blue to red from the N-terminus to the C-terminus, respectively. The view is down the b axis (unit cell shown in magenta), showing four molecules in the asymmetric unit.

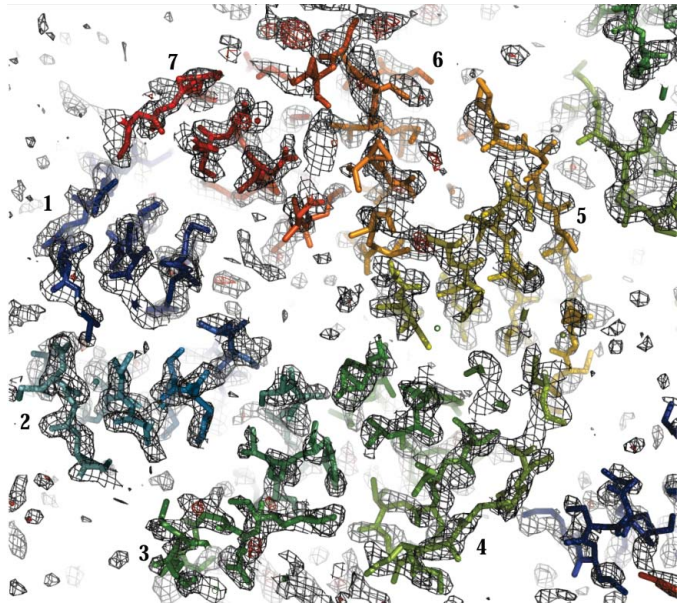

Figure 5
The $2F_o - F_c$ (grey) and $F_o - F_c$ (red, positive) electron-density maps for the current model of YncE-His$_6$ (residues 22–323) contoured at 1σ and 3σ, respectively, calculated using *NCSREF*. The R and R_{free} for the current model are 41.1% and 51.5%, respectively, following ten cycles of restrained refinement using *REFMAC*. The view and labelling are similar to those in Fig. 4, highlighting the β-propeller fold and showing clear secondary-structural features for the majority of the protein. Manual rebuilding and refinement are in progress.

The structure solution was obtained using *Phaser* (Fig. 4), based on a model derived from the β-propeller domain of the archeal surface-layer protein (PDB code 1l0q). The program *DM* (Cowtan & Main, 1996) was used for noncrystallographic symmetry (NCS) averaging and solvent flattening of the electron-density map (as implemented in the *CCP*4 program *NCSREF*). The resulting electron-density map clearly shows distinguishable secondary-structural features for at least 70% of the protein (Fig. 5). The R factor and $R_{\rm free}$ for the current model (residues 22–323) are 41.1% and 51.5%, respectively. The two C-terminal blades of the β-propeller structure show the most poorly defined density; consequently, iterative manual rebuilding and maximum-likelihood refinement are in progress using the programs *Coot* (Emsley & Cowtan, 2004) and *REFMAC* (Murshudov *et al.*, 1997), respectively.

The crystal structure of YncE is only the second structurally characterized protein belonging to the YVTN β-propeller family and confirms the presence of a single β-propeller domain that contains seven four-stranded β-sheets. The completed YncE structure will allow comparisons with other members of the β-propeller superfamily, which will provide insights into the possible molecular function of this protein as well as those of other YVTN β-propeller proteins.

The authors wish to express their thanks to the staff at SRS Daresbury for providing excellent beamline facilities and support. This work was supported by the Lister Institute of Preventive Medicine (personal fellowship to KAW), the BBSRC (project grant to SCA) and the Borno State Scholarship Board (studentship to AB-D).

References

Baars, L., Ytterberg, A. J., Drew, D., Wagner, S., Thilo, C., van Wijk, K. J. & de Gier, J. W. (2006). *J. Biol. Chem.* **281**, 10024–10034.
Collaborative Computational Project, Number 4 (1994). *Acta Cryst.* D**50**, 760–763.
Cowtan, K. D. & Main, P. (1996). *Acta Cryst.* D**52**, 43–48.
Emsley, P. & Cowtan, K. (2004). *Acta Cryst.* D**60**, 2126–2132.
Evans, P. (1997). *Jnt CCP4/ESF–EACBM Newsl. Protein Crystallogr.* **33**, 22–24.
Jing, H., Takagi, J., Liu, J. H., Lindgren, S., Zhang, R. G., Joachimiak, A., Wang, J. H. & Springer, T. A. (2002). *Structure*, **10**, 1453–1464.
Leslie, A. G. W. (1992). *Jnt CCP4/ESF–EACBM Newsl. Protein Crystallogr.* **26**.
McCoy, A. J., Grosse-Kunstleve, R. W., Adams, P. D., Winn, M. D., Storoni, L. C. & Read, R. J. (2007). *J. Appl. Cryst.* **40**, 658–674.
McHugh, J. P., Rodriguez-Quinones, F., Abdul-Tehrani, H., Svistunenko, D. A., Poole, R. K., Cooper, C. E. & Andrews, S. C. (2003). *J. Biol. Chem.* **278**, 29478–29486.
Murshudov, G. N., Vagin, A. A. & Dodson, E. J. (1997). *Acta Cryst.* D**53**, 240–255.
Nataro, J. P., Seriwatana, J., Fasano, A., Maneval, D. R., Guers, L. D., Noriega, F., Dubovsky, F., Levine, M. M. & Morris, J. G. Jr (1995). *Infect. Immun.* **63**, 4721–4728.
Šmajs, D. & Weinstock, G. M. (2001). *J. Bacteriol.* **183**, 3958–3966.